



HAL
open science

The crystal structure of the catalytic domain of the Ser/Thr kinase PknA from *M. tuberculosis* shows an Src-like autoinhibited conformation

Tristan Wagner, Matthieu Alexandre, Rosario Duran, Nathalie Barilone, Annemarie Wehenkel, Pedro M. Alzari, Marco Bellinzoni

► To cite this version:

Tristan Wagner, Matthieu Alexandre, Rosario Duran, Nathalie Barilone, Annemarie Wehenkel, et al.. The crystal structure of the catalytic domain of the Ser/Thr kinase PknA from *M. tuberculosis* shows an Src-like autoinhibited conformation. *Proteins - Structure, Function and Bioinformatics*, 2015, 83 (5), pp.982-988. 10.1002/prot.24754 . pasteur-01175001

HAL Id: pasteur-01175001

<https://pasteur.hal.science/pasteur-01175001>

Submitted on 10 Jul 2015

HAL is a multi-disciplinary open access archive for the deposit and dissemination of scientific research documents, whether they are published or not. The documents may come from teaching and research institutions in France or abroad, or from public or private research centers.

L'archive ouverte pluridisciplinaire **HAL**, est destinée au dépôt et à la diffusion de documents scientifiques de niveau recherche, publiés ou non, émanant des établissements d'enseignement et de recherche français ou étrangers, des laboratoires publics ou privés.



Distributed under a Creative Commons Attribution - NonCommercial - NoDerivatives 4.0 International License



The crystal structure of the catalytic domain of the Ser/Thr kinase PknA from *M. tuberculosis* shows an Src-like autoinhibited conformation

Journal:	<i>PROTEINS: Structure, Function, and Bioinformatics</i>
Manuscript ID:	Prot-00517-2014.R1
Wiley - Manuscript type:	Structure Note
Date Submitted by the Author:	n/a
Complete List of Authors:	Wagner, Tristan; Max Planck Institute for Terrestrial Microbiology, - Alexandre, Matthieu; Institut Pasteur, Structural Biology and Chemistry Duran, Rosario; Institut Pasteur de Montevideo, Analytical Biochemistry and Proteomics Barilone, Nathalie; Institut Pasteur, Viral Neuroimmunology Wehenkel, Annemarie; Institut Curie, Signalling, Neurobiology and Cancer Alzari, Pedro; Institut Pasteur, CNRS URA 359, Unite de Biochimie Structurale; Bellinzoni, Marco; Institut Pasteur, Structural Biology and Chemistry
Key Words:	Mycobacterium tuberculosis, Ser/Thr phosphorylation, Autophosphorylation, Autoinhibition, X-ray crystallography, Mass spectrometry

SCHOLARONE™
Manuscripts

1
2
3 **The crystal structure of the catalytic domain of the Ser/Thr kinase PknA from**
4
5 ***M. tuberculosis* shows an Src-like autoinhibited conformation**
6
7

8
9 Tristan Wagner^{1,2,3§}, Matthieu Alexandre^{1,2,3}, Rosario Duran^{4,5}, Nathalie Barilone^{1,2,3§},
10
11 Annemarie Wehenkel^{1,2,3§}, Pedro M. Alzari^{1,2,3}, Marco Bellinzoni^{1,2,3*}
12
13

14
15
16
17
18 ¹ Institut Pasteur, Unité de Microbiologie Structurale, 75724 Paris, France; ² CNRS
19
20 UMR 3528, 75724 Paris, France; ³ Université Paris Diderot, Sorbonne Paris Cité,
21
22 Microbiologie Structurale, 75724 Paris, France; ⁴ Unidad de Bioquímica y Proteómica
23
24 Analíticas, Institut Pasteur de Montevideo, Uruguay; ⁵ Unidad de Bioquímica y
25
26 Proteómica Analíticas, Instituto de Investigaciones Biológicas Clemente Estable,
27
28 Ministerio de Educación y Cultura, Uruguay.
29
30
31

32
33
34
35
36 Short Title: Structure of the Ser/Thr protein kinase PknA
37

38
39 Keywords: *Mycobacterium tuberculosis*, Ser/Thr phosphorylation,
40
41 autophosphorylation, autoinhibition, X-ray crystallography, mass spectrometry.
42
43

44
45 * Corresponding author: Marco Bellinzoni, marco.bellinzoni@pasteur.fr
46

47
48 § Present address: TW: Max Planck Institute for Terrestrial Microbiology, Karl-von-
49
50 Frisch-Straße, 35043 Marburg, Germany; NB: Institut Pasteur, Unité de Neuro-
51
52 Immunologie Virale, 75724 Paris cedex 15, France; AW: Institut Curie, 91405 Orsay,
53
54 France
55
56
57
58
59
60

ABSTRACT

Signal transduction mediated by Ser/Thr phosphorylation in *Mycobacterium tuberculosis* has been intensively studied in the last years, as its genome harbors eleven genes coding for eukaryotic-like Ser/Thr kinases. Here we describe the crystal structure and the autophosphorylation sites of the catalytic domain of PknA, one of two protein kinases essential for pathogen's survival. The structure of the ligand-free kinase domain shows an auto-inhibited conformation similar to that observed in human Tyr kinases of the Src-family. These results reinforce the high conservation of structural hallmarks and regulation mechanisms between prokaryotic and eukaryotic protein kinases.

1
2
3 Originally thought to be restricted to the eukaryotic kingdom, reversible protein
4 phosphorylation on serine, threonine and tyrosine residues has emerged as a
5 widespread signaling mechanism in prokaryotes and has turned into a highly active
6 field of research in modern molecular microbiology. *Mycobacterium tuberculosis* was
7 among the first microorganisms for which genomic data indicated the presence of
8 eukaryotic-like Ser/Thr kinases (STPKs) and has been intensively studied since, given
9 the high interest in STPKs as possible targets for the development of new anti-
10 tuberculosis drugs ^{1, 2}. PknA is found together with a second kinase, PknB, in a
11 conserved operon that also includes two genes coding for FHA domain proteins
12 (FhaA and FhaB), a penicillin-binding protein (PbpA), a putative cell division protein
13 (RodA), and the only known Ser/Thr phosphatase (PstP) of the *M. tuberculosis*
14 genome ^{1, 2}. The two kinases, PknA and PknB, are thought to be involved in the
15 control of cell division and were shown to be essential for mycobacterial growth ².
16 Although PknB is one of the most studied eukaryotic-like bacterial kinases and the
17 first for which the crystal structure became available ¹, the detailed signaling
18 pathway(s) in which these STPKs could be involved remain elusive. Moreover, in
19 contrast to PknB, for which structural and biochemical evidence has started to shed
20 light on its regulation mechanisms ³, the absence of structural data for PknA has
21 hampered further functional studies, despite the likely involvement of this kinase in
22 common signaling pathways. We describe here the crystal structure of the catalytic
23 domain of PknA and the identification of several autophosphorylation sites in the
24 intracellular region, providing first clues about the regulation mechanism of this
25 essential mycobacterial kinase.
26
27
28
29
30
31
32
33
34
35
36
37
38
39
40
41
42
43
44
45
46
47
48
49
50
51
52

53 54 55 56 **MATERIALS AND METHODS** 57 58 59 60

1
2
3 ***Cloning, expression and purification.*** To produce recombinant soluble protein for
4 structural studies, the portion of the *pknA* gene (rv0015c) coding for the predicted
5 intracellular moiety (PknA₁₋₃₃₆) was amplified by PCR from the cosmid
6 MTCY10H4, introducing a 5' DNA sequence coding for the TEV protease cleavage
7 site (ENLYFQG), as well as a *EcoRI* restriction site at both ends. The purified PCR
8 fragment was then cloned in the pET-28a vector leading to plasmid pM260, which
9 was subsequently used to transform the *E. coli* strain BL21(DE3)pLysS for protein
10 production. The transformed strain was grown at 30°C in LB medium supplemented
11 with 50 µg/ml kanamycin and 30 µg/ml chloramphenicol, and protein overexpression
12 was achieved by induction with 1 mM IPTG once OD₆₀₀ ~ 0.7, followed by 3.0 h
13 growth at 30°C. Cells were then harvested by centrifugation, washed with PBS (140
14 mM NaCl, 2.7 mM KCl, 10 mM Na₂HPO₄, 1.8 mM KH₂PO₄, pH 7.3) and frozen at -
15 80°C. Pellets were thawed, resuspended in lysis buffer (50 mM NaH₂PO₄, 500 mM
16 NaCl, 25 mM imidazole, 5% glycerol; pH 8.0) and lysed by sonication on ice;
17 lysates were then centrifuged at 26,800 x g for 1 h, filtered on a 0.45 µm membrane
18 and loaded with a peristaltic pump onto a 1 ml HisTrap Ni²⁺-IMAC column (GE
19 Healthcare). PknA₁₋₃₃₆ was eluted applying a 25-400 mM imidazole gradient in the
20 same buffer; the fractions containing the recombinant protein, as confirmed by 12%
21 SDS-PAGE, were pooled and dialysed overnight at 18°C against a specific PknA
22 buffer (25 mM Hepes-Na pH 8.0, 500 mM NaCl, 5% glycerol, 1 mM DTT). During
23 the dialysis a recombinant His₆-tagged TEV protease was added to a 1:35 w/w ratio.
24 The dialyzed sample was passed by gravity flow through 1.0 ml of Ni-NTA resin
25 (Qiagen) in order to eliminate the TEV protease and the cleaved His₆ expression tag,
26 eluted with 3 ml of PknA buffer supplemented with 50 mM imidazole, concentrated
27 and injected onto a HiLoad 16/60 Superdex 75 size exclusion column (GE
28
29
30
31
32
33
34
35
36
37
38
39
40
41
42
43
44
45
46
47
48
49
50
51
52
53
54
55
56
57
58
59
60

1
2
3 Healthcare), equilibrated in the PknA buffer (with no imidazole) and run at 1 ml/min.
4
5 Peak fractions containing PknA₁₋₃₃₆ were pooled and concentrated up to 36 mg/ml
6
7 with a 10 kDa-cut off Vivaspin concentrator (Sartorius). The concentrated protein,
8
9 with a purity > 95% as estimated by Coomassie blue staining on SDS-PAGE, was
10
11 flash-frozen in liquid nitrogen and stored at -80°C.
12
13

14
15
16 ***Phosphorylation site identification by tandem mass spectrometry.*** Protein samples
17
18 were digested with different proteolytic enzymes (chymotrypsin, trypsin and
19
20 endoproteinase GluC) by incubation overnight at 37°C. The resulting peptides were
21
22 separated using a nano-HPLC system (Proxeon EasynLC, Thermo) fitted with a
23
24 reverse-phase column (easy C18 column, 3 µm; 75 µm ID×10 cm; Proxeon, Thermo)
25
26 eluted with a 0.1% (v/v) formic acid in a water to acetonitrile gradient (0–35%
27
28 acetonitrile in 40 min; flow 400 nl/min). Online MS analysis was carried out in the
29
30 LTQ Velos nano-ESI-linear ion trap instrument (Thermo) in data dependent
31
32 acquisition mode (full scan followed by MS/MS of the top 5 peaks in each segment,
33
34 using a dynamic exclusion list). Peptide sequences were assigned using Mascot and
35
36 Sequest search engines. An in-house Mascot v.2.0 version was used for searching the
37
38 Swissprot database (20121102) with the following parameters: taxonomy:
39
40 *Mycobacterium tuberculosis* complex; peptide tolerance: 1.5 Da; MS/MS tolerance:
41
42 0.8 Da; methionine oxidation, and Ser/Thr phosphorylation as the allowed variable
43
44 modifications. The data was filtered using significance threshold p<0.05 and ion
45
46 score>30. In addition raw MS/MS spectra were interpreted with the Proteome
47
48 Discoverer software package (v.1.3.0.339, Thermo). We considered positive
49
50 phosphosite identification when more than one spectra for the phosphopeptide was
51
52
53
54
55
56
57
58
59
60

1
2
3 obtained, pRS probability was >95% and manual inspection of the MS/MS spectra
4
5 showed at least two confirmatory fragment ions.
6
7

8
9
10 **Crystallization.** Initial crystallization screenings of PknA₁₋₃₃₆ were carried out at 18°C
11
12 by the sitting drop method in a 96-well format (200+200 nl drops dispensed by a
13
14 Cartesian nanolitre system). Microcrystals were identified in a crystallization
15
16 condition containing 4.3 M NaCl, 100 mM Hepes-Na pH 8.0, which was refined in
17
18 several steps by preparing hand-made hanging drops in 24-well plates at the same
19
20 temperature. The final crystallization buffer was 3.8 M NaCl, 100 mM MES pH 6.7,
21
22 14.3 mM Na acetate pH 4.5, with which crystals suitable to structural determination
23
24 grew in 8 to 10 days by microseeding from the original condition. Crystals were flash-
25
26 frozen in liquid nitrogen after quick soaking in a cryoprotectant mixture made of 75%
27
28 crystallization solution and 25% glycerol.
29
30
31

32
33
34 **Data collection, structure determination and refinement.** X-ray diffraction data were
35
36 collected at 100 K on the beamline ID14-2 at the European Synchrotron Radiation
37
38 Facility (ESRF) (Grenoble, France). The structure was solved by molecular
39
40 replacement with Phaser⁴, using the split N-terminal (residues 5-97) and C-terminal
41
42 (residues 99-276) domains of the STPK PknB from *M. tuberculosis* (pdb entry 1o6y;
43
44 ⁵) as separate search models. The molecular replacement solution, composed of three
45
46 kinase domains per asymmetric unit, was refined with either refmac5⁶ or
47
48 autoBUSTER, applying local structure similarity restraints for NCS⁷. The model was
49
50 validated through the Molprobit server⁸. **Figures were generated and rendered with**
51
52 **PyMOL (The PyMOL Molecular Graphics System, Version 1.5, Schrödinger, LLC).**
53
54
55
56
57
58
59
60

Coordinates and structure factors have been deposited in the pdb under the accession code 4X3F.

RESULTS AND DISCUSSION

Overall structure. Although attempts to overexpress the N-terminal catalytic domain (residues 1-276) of PknA in *E. coli* were unsuccessful, we were able to express and purify the whole intracellular moiety of the kinase, including the entire juxtamembrane segment (residues 277-336), as a His₆-tagged soluble protein to a satisfactory yield (~ 3.5 mg/l of culture). This construct is active on the FHA domain substrate GarA, as reported⁹. After proteolytic removal of the affinity tag, the recombinant protein crystallized in high salt conditions (around 4 M NaCl). The crystals belong to the monoclinic space group C2 and the 3D structure has been determined to 2.9 Å using molecular replacement methods (Table 1). The asymmetric unit contains three molecules of PknA, all of which were traceable from the N-terminus (with the exception of Met1 and Ser2, not visible in all chains) to residue Pro289, corresponding to the whole catalytic domain plus the first 13 residues of the juxtamembrane segment. In contrast, no supporting electron density was observed for the remaining part of the juxtamembrane segment (residues Gly290 to Gly336). The catalytic domain shows the canonical, bi-lobal protein kinase fold, with an N-terminal lobe (Met1 to Val98), composed of a five-stranded antiparallel β-sheet plus the functionally important αC helix (Pro52 to Ala66), followed by a mostly α-helical C-terminal lobe (residues Asn98 to Gly277) that includes helices αD to αI (**Fig. 1A**). Just outside the catalytic domain, the N-terminal visible portion of the juxtamembrane segment makes a left-handed PPII helix extension to the C-terminal lobe of the kinase (**Fig. 1B**). This segment makes two H-bonds with the catalytic domain, one between

1
2
3 the amide nitrogen of Arg278 and the carbonyl oxygen of Ala273 (at the end of the
4
5 helix α I), the other between the carbonyl of Pro281 and the hydroxyl of Tyr 261 in
6
7 the α G to α I linker. In contrast to earlier reports ¹⁰, the mostly disordered
8
9 juxtamembrane region of PknA suggests that this region might be dispensable for
10
11 enzymatic activity. In agreement with this hypothesis, we observed that a shorter
12
13 PknA construct lacking most of the juxtamembrane segment, PknA₁₋₂₉₀, was indeed
14
15 capable of phosphorylating the substrate GarA (data not shown).
16
17

18
19
20
21 Despite our attempts to get co-crystals of PknA with commercially available non-
22
23 hydrolysable ATP analogs, the catalytic site, situated at the interface between the two
24
25 lobes as in all Ser/Thr and Tyr protein kinases, shows no bound nucleotide or divalent
26
27 ion. Nevertheless, the ensemble of well-documented elements of Hanks-type kinases
28
29 is easily identifiable. The activation loop is comprised of 28 residues between the
30
31 sequence motifs DFG (Asp159-Phe160-Gly161) and APE (Ala185-Pro186-Glu187),
32
33 two of the extremely conserved features of protein kinases (**Fig. 1C; Fig. 2A**). Among
34
35 the other traits of Hanks-type kinases, the conserved lysine on the β 3 strand (Lys42),
36
37 involved in the binding of the ATP α and β phosphates, the equally conserved
38
39 glutamate on the critical α C helix (Glu61), involved in the correct positioning of the
40
41 same lysine by a salt bridge, and the so-called HRD motif (His139-Arg140-Asp141)
42
43 that identifies the catalytic loop and allow to classify PknA as an RD-kinase (**Fig.**
44
45 **2A**). However, the whole activation loop and part of the following P+1 loop are
46
47 disordered in each of the three chains in the asymmetric unit, as judged by the lack of
48
49 supporting electron density for residues 168-177 (chain A), 164-174 (chain B), 164-
50
51 175 (chain C).
52
53
54
55
56
57
58
59
60

1
2
3 ***PknA autophosphorylation.*** The autophosphorylation pattern of PknA was analyzed
4
5 by mass spectrometry. The protein shows a heterogenous phosphorylation pattern
6
7 with multiple sites identified in good agreement with previous results for PknA and
8
9 other mycobacterial Ser/Thr protein kinases ^{11, 12}. MS/MS analysis of the PknA tryptic
10
11 digest allowed to detect 21 phosphorylated peptides and to identify 18
12
13 phosphorylation sites (**Supplementary Table 1**). For two phosphopeptides (sequence
14
15 292-304 and 279-291), the phosphoresidue location could not be unambiguously
16
17 determined (**Supplementary Table 1**). However, no tryptic peptides corresponding to
18
19 the activation loop sequence could be identified. To increase sequence coverage and
20
21 improve phosphosite identification, we digested PknA with different proteolytic
22
23 enzymes. Both chymotryptic and endoproteinase GluC digests confirmed some of the
24
25 previously identified phosphoresidues (data not shown) and led to further
26
27 identification of new sites (**Supplementary Table 1**). In particular, a triply charged
28
29 ion (m/z 1441.71) could be assigned to a peptide (residues 160-199) containing four
30
31 phosphorylated residues and one methionine oxidation with a significant Mascot ion
32
33 score (experimental M_r = 4322.11, calculated M_r = 4321.78). This segment, which
34
35 overlaps with the kinase activation loop, includes the highly conserved Thr residues
36
37 whose phosphorylation was important for activation in other mycobacterial Ser/Thr
38
39 protein kinases ¹². However, the fragmentation properties of this multiply
40
41 phosphorylated peptide preclude the detection of sequence-specific ion signals, thus
42
43 rendering the localization of phosphorylated sites difficult.
44
45
46
47
48
49
50
51

52 In a previous report, eight phosphorylation sites were identified in PknA₁₋₃₃₈ ¹¹.
53
54 Except for Ser212, all the other sites were also detected in our experimental
55
56 conditions. In addition we report 12 new phosphorylation sites and provide evidence
57
58
59
60

1
2
3 supporting the presence of multiple phosphorylation sites in the activation loop,
4
5 although the exact sites could not be unambiguously assigned. It should be noted that
6
7 only four of these phosphoresidues (Thr21, Ser46, Thr152, Thr224) were visible in
8
9 the electron density maps of at least one PknA molecule, but they are highly exposed
10
11 to solvent and possibly do not play a regulatory or structural role.
12
13

14
15
16 ***PknA displays an autoinhibited state.*** The relative position of the two lobes suggests
17
18 that PknA has been crystallized in a closed state, as observed for PknB in complex
19
20 with nucleotides or for the ternary complex of human PKA (pdb entry 1atp) (**Fig. 2B**),
21
22 generally considered as the prototype of the active form of Ser/Thr kinases ¹³. The
23
24 plasticity of the activation loop and lack of supporting electron density is similar to
25
26 what is observed for the active conformation of the related *M. tuberculosis* Ser/Thr
27
28 kinase PknB, as reported independently by different teams ². However, the
29
30 conformation of PknA corresponds to an inactive state, close to the autoinhibited
31
32 structure of the kinase domain of *Staphylococcus aureus* PknB (**Fig. 2B**) (pdb entry
33
34 4eqm; ¹⁴). Furthermore, the N-terminus of PknA helix α C is rotated approximately
35
36 17° outwards of the active site pocket with respect to the same helix in PknB,
37
38 hampering formation of the salt bridge Glu61 - Lys42 that is a hallmark of active
39
40 protein kinases (**Fig. 2B**). A similar, but less pronounced tilt of α C was also observed
41
42 in the inactive conformation of mycobacterial PknE (pdb entry 2h34) (**Fig. 2B**).
43
44
45
46
47
48
49

50 Noteworthy, the conformation of apo PknA represents an example of the well-
51
52 characterized CDK/Src-like inactive conformation, observed in a number of structures
53
54 of both Ser/Thr and Tyr kinases (reviewed in ¹⁵). The known features of this
55
56 autoinhibited conformation include the closure of the lobes and the swinging out of
57
58
59
60

1
2
3 α C. Furthermore, the N-terminal portion of the activation loop (residues Ile162 to
4 Asp167 in PknA), which immediately follows the DFG motif, assumes a well defined
5 one-turn helical conformation that packs against α C, stabilizing its outward
6 orientation and creating a barrier to the Lys-Glu salt bridge (**Fig. 2A**). The presence of
7 such an inhibitory helix (or A-loop helix for activation loop) was first observed in the
8 crystal structures of the human tyrosine kinases c-Src in complex with AMP-PNP
9 (pdb entry 2src; ¹⁶), as well as Hrc in complex with the pyrazolo-pyrimidine inhibitor
10 PP1 (pdb entry 1qcf; ¹⁷). In chains B and C of PknA, however, a slightly different
11 autoinhibited conformation is observed, with the traceable residues of the activation
12 loop, despite not forming an α -helix, still hindering the Lys-Glu interaction and the
13 carboxylic group of Glu61 positioned instead to form a salt bridge with the
14 guanidinium of Arg140, part of the HRD motif and adjacent to the strictly conserved
15 Asp141 within the catalytic loop. This interaction, that contributes to stabilizing the
16 α C outward orientation, was also observed in the two tyrosine kinases mentioned
17 above and has recently been proposed to represent an intermediate state through the
18 path to the active conformation ¹⁵. Consistently with the present crystal structure of
19 PknA representing an inactive conformation, the catalytic and regulatory spines (two
20 conserved intramolecular networks between the N- and C-lobes in active protein
21 kinases ¹⁸) are also not properly assembled.

22
23
24
25
26
27
28
29
30
31
32
33
34
35
36
37
38
39
40
41
42
43
44
45
46
47
48 ***A conserved activation mechanism in mycobacterial kinases?*** The crystal structures
49 of the catalytic domains of PknB and PknE, the two other *M. tuberculosis* predicted
50 receptor kinases for which a three-dimensional structure of the kinase domain is
51 available, showed in both cases an homodimeric form referred to as 'back-to-back',
52 since the dimerization interface involves the N-terminal lobe surface located opposite
53
54
55
56
57
58
59
60

1
2
3 to the active site ². This ‘back-to-back’ dimerization has been proposed to act as a
4
5 general allosteric activation mechanism in receptor-like mycobacterial kinases ³, in
6
7 which homodimer formation is required in order to achieve activation loop
8
9 phosphorylation and kinase activation. A similar mechanism might also be
10
11 operational in PknA, since the equivalent N-terminal homodimerization interface is
12
13 well conserved (**Supplementary Figure 1**) and the activation loop has several
14
15 phosphorylation sites. However, further experimental evidence is necessary to
16
17 validate this model or, alternatively, support the recently postulated existence of a
18
19 hierarchical kinase network in *M. tuberculosis*, according to which phosphorylation
20
21 by PknB would be required for PknA activation ⁹.
22
23
24
25
26

27 **ACKNOWLEDGEMENTS**

28
29 We are grateful to Clément Moroldo for generating and testing constructs for
30
31 recombinant protein expression, to Ahmed Haouz and Patrick Weber for robot-driven
32
33 crystallization screenings, and to Gwénaëlle André-Leroux and María-Natalia Lisa for
34
35 many helpful discussions. The expression plasmid for the TEV protease was a kind
36
37 gift from Helena Berglund (Karolinska Institute, Stockholm, Sweden). We also
38
39 acknowledge the ESRF (Grenoble, France) for granting access to its macromolecular
40
41 crystallography facilities. This work has been funded by grants from the Institut
42
43 Pasteur, the CNRS and the European Commission (contract number LSHP-CT-2005-
44
45 018923).
46
47
48
49
50

51 **REFERENCES**

- 52
53
54 1. Wehenkel A, Bellinzoni M, Graña M, Duran R, Villarino A, Fernandez P,
55
56 Andre-Leroux G, England P, Takiff H, Cerveñansky C, Cole ST, Alzari PM.
57
58
59
60

- 1
2
3 Mycobacterial Ser/Thr protein kinases and phosphatases: physiological roles
4 and therapeutic potential. *Biochim Biophys Acta* 2008;1784:193–202.
5
6
7 2. Pristic S, Husson RN. *Mycobacterium tuberculosis* Serine/Threonine Protein
8 Kinases. *Microbiol Spectr* 2014;2.
9
10
11 3. Lombana TN, Echols N, Good MC, Thomsen ND, Ng H-L, Greenstein AE,
12 Falick AM, King DS, Alber T. Allosteric activation mechanism of the
13 *Mycobacterium tuberculosis* receptor Ser/Thr protein kinase, PknB. *Structure*
14 2010;18:1667–1677.
15
16
17 4. McCoy AJ, Grosse-Kunstleve RW, Adams PD, Winn MD, Storoni LC, Read
18 RJ. Phaser crystallographic software. *J Appl Crystallogr* 2007;40:658–674.
19
20
21 5. Ortiz-Lombardía M, Pompeo F, Boitel B, Alzari PM. Crystal structure of the
22 catalytic domain of the PknB serine/threonine kinase from *Mycobacterium*
23 *tuberculosis*. *J Biol Chem* 2003;278:13094–13100.
24
25
26 6. Murshudov GN, Skubak P, Lebedev AA, Pannu NS, Steiner RA, Nicholls RA,
27 Winn MD, Long F, Vagin AA. REFMAC5 for the refinement of
28 macromolecular crystal structures. *Acta Crystallogr D Biol Crystallogr*
29 2011;67:355–367.
30
31
32 7. Smart OS, Womack TO, Flensburg C, Keller P, Paciorek W, Sharff A,
33 Vonrhein C, Bricogne G. Exploiting structure similarity in refinement:
34 automated NCS and target-structure restraints in BUSTER. *Acta Crystallogr D*
35 *Biol Crystallogr* 2012;68:368–380.
36
37
38 8. Chen VB, Arendall WB3, Headd JJ, Keedy DA, Immormino RM, Kapral GJ,
39 Murray LW, Richardson JS, Richardson DC. MolProbity: all-atom structure
40 validation for macromolecular crystallography. *Acta Crystallogr D Biol*
41 *Crystallogr* 2010;66:12–21.
42
43
44
45
46
47
48
49
50
51
52
53
54
55
56
57
58
59
60

- 1
2
3 9. Baer CE, Iavarone AT, Alber T, Sasseti CM. Biochemical and Spatial
4
5 Coincidence in the Provisional Ser/Thr Protein Kinase Interaction Network of
6
7 *Mycobacterium tuberculosis*. J Biol Chem 2014;289:20422–20433.
8
- 9
10 10. Thakur M, Chaba R, Mondal AK, Chakraborti PK. Interdomain interaction
11
12 reconstitutes the functionality of PknA, a eukaryotic type Ser/Thr kinase from
13
14 *Mycobacterium tuberculosis*. J Biol Chem 2008;283:8023–8033.
15
- 16
17 11. Molle V, Zanella-Cleon I, Robin J-P, Mallejac S, Cozzone AJ, Becchi M.
18
19 Characterization of the phosphorylation sites of *Mycobacterium tuberculosis*
20
21 serine/threonine protein kinases, PknA, PknD, PknE, and PknH by mass
22
23 spectrometry. Proteomics 2006;6:3754–3766.
24
- 25
26 12. Duran R, Villarino A, Bellinzoni M, Wehenkel A, Fernandez P, Boitel B, Cole
27
28 ST, Alzari PM, Cerveñansky C. Conserved autophosphorylation pattern in
29
30 activation loops and juxtamembrane regions of *Mycobacterium tuberculosis*
31
32 Ser/Thr protein kinases. Biochem Biophys Res Commun 2005;333:858–867.
33
- 34
35 13. Knighton DR, Zheng JH, Eyck Ten LF, Ashford VA, Xuong NH, Taylor SS,
36
37 Sowadski JM. Crystal structure of the catalytic subunit of cyclic adenosine
38
39 monophosphate-dependent protein kinase. Science 1991;253:407–414.
40
- 41
42 14. Raketts S, Donat S, Ohlsen K, Stehle T. Structural Analysis of *Staphylococcus*
43
44 *aureus* Serine/Threonine Kinase PknB. PLoS One 2012;7:e39136.
45
- 46
47 15. Jura N, Zhang X, Endres NF, Seeliger MA, Schindler T, Kuriyan J. Catalytic
48
49 Control in the EGF Receptor and Its Connection to General Kinase Regulatory
50
51 Mechanisms. Mol Cell 2011;42:9–22.
52
- 53
54 16. Xu W, Doshi A, Lei M, Eck MJ, Harrison SC. Crystal structures of c-Src
55
56 reveal features of its autoinhibitory mechanism. Mol Cell 1999;3:629–638.
57
- 58
59 17. Schindler T, Sicheri F, Pico A, Gazit A, Levitzki A, Kuriyan J. Crystal
60

1
2
3 structure of Hck in complex with a Src family-selective tyrosine kinase
4 inhibitor. *Mol Cell* 1999;3:639–648.
5
6

- 7 18. Kornev AP, Taylor SS. Defining the conserved internal architecture of a
8 protein kinase. *Biochim Biophys Acta* 2010;1804:440–444.
9
10 19. Robert X, Gouet P. Deciphering key features in protein structures with the new
11 ENDscript server. *Nucleic Acids Res* 2014;42:W320–W324.
12
13 20. Gay LM, Ng H-L, Alber T. A conserved dimer and global conformational
14 changes in the structure of apo-PknE Ser/Thr protein kinase from
15 *Mycobacterium tuberculosis*. *J Mol Biol* 2006;360:409–420.
16
17
18
19
20
21
22
23
24
25
26
27
28
29
30
31
32
33
34
35
36
37
38
39
40
41
42
43
44
45
46
47
48
49
50
51
52
53
54
55
56
57
58
59
60

FIGURE LEGENDS

Fig. 1. (A, B) Cartoon representation of the overall structure of the catalytic domain of PknA in unliganded form; secondary structure elements are indicated. The modeled portion of the juxtamembrane segment, which folds as a left-handed PPII helix, is shown in orange. The phosphorylated residues identified in electron density maps are indicated. **(C)** Sequence alignment of the N-terminal catalytic domains of the transmembrane receptor *M. tuberculosis* kinases PknA, PknB, PknD, PknE, PknF, PknH, PknI, PknJ, PknL that all share the same domain topology^{1, 2, 9}; PknG and PknK, which are soluble kinases, are omitted. The secondary structure elements of the catalytic domain of PknA (this work) have been depicted through ESPript 3.0¹⁹.

Fig. 2. (A) Close view of the active site pocket in PknA. The activation segment is highlighted in orange, and key conserved residue motifs known to be involved in the phosphorylation process or in structuring a catalytically competent kinase are shown in sticks, i.e. the motifs HRD (His139 to Asp141), DFG (Asp159 to Gly161), APE (Ala185 to Glu187). The N-terminal modeled portion of the activation loop, which is structured as a one-turn inhibitory α -helix packing against α C, is shown in red. The unassembled catalytic and regulatory spines (C-spine in light brown, R-spine in yellow) are shown with a semitransparent surface representation. See the text for details. **(B)** Lateral view of the superimposed catalytic domains of PknA (yellow, this study), *M. tuberculosis* PknB in complex with AMP-PCP (pdb entry 1o6y, light brown;⁵), *M. tuberculosis* PknE (green; pdb entry 2h34,²⁰), *S. aureus* PknB (gray; pdb entry 4eqm,¹⁴) and the human cAMP-dependent kinase PKA in ternary complex with MgATP and an inhibitory peptide, shown as the paradigm of the active conformation of a Hanks-type protein kinase (purple; pdb entry 1atp,¹³). The dashed

lines indicate the different orientation of the α C helix axis when comparing PknA (yellow) and PknB (light brown).

For Peer Review

1
2
3
4
5
6
7
8
9
10
11
12
13
14
15
16
17
18
19
20
21
22
23
24
25
26
27
28
29
30
31
32
33
34
35
36
37
38
39
40
41
42
43
44
45
46
47
48
49
50
51
52
53
54
55
56
57
58
59
60

Table 1. Crystallographic data collection and refinement statistics. Values relative to the highest resolution shell are within parentheses.

	His₆-tagged SeMet-labelled, centred monoclinic
Data collection	
Synchrotron beamline	ESRF ID14-2
Wavelength (Å)	0.933
Space group	C2
Cell dimensions <i>a</i> , <i>b</i> , <i>c</i> (Å)	102.31, 150.18, 96.54
α , β , γ (°)	90.0, 96.98, 90.0
Resolution (Å)	43.57 – 2.90 (3.06 – 2.90)
<i>R</i> _{merge}	0.107 (1.197)
<i>I</i> / σ (<i>I</i>)	8.3 (1.1)
CC(1/2) (%)	99.5 (47.1)
Unique reflections	31961
Completeness (%)	99.6 (99.1)
Redundancy	3.6 (3.5)
Refinement	
Resolution (Å)	37.98 – 2.90
No. reflections*	30353
<i>R</i> _{work} / <i>R</i> _{free} (%)	21.9/24.3
Average B-factors (Å ²)	95.1
Macromolecule	95.1
Solvent	54.7
R.m.s deviations	
Bond lengths (Å)	0.010
Bond angles (°)	1.289
PDB #	4X3F

* Excluding the *R*_{free} set (5% of total reflections).

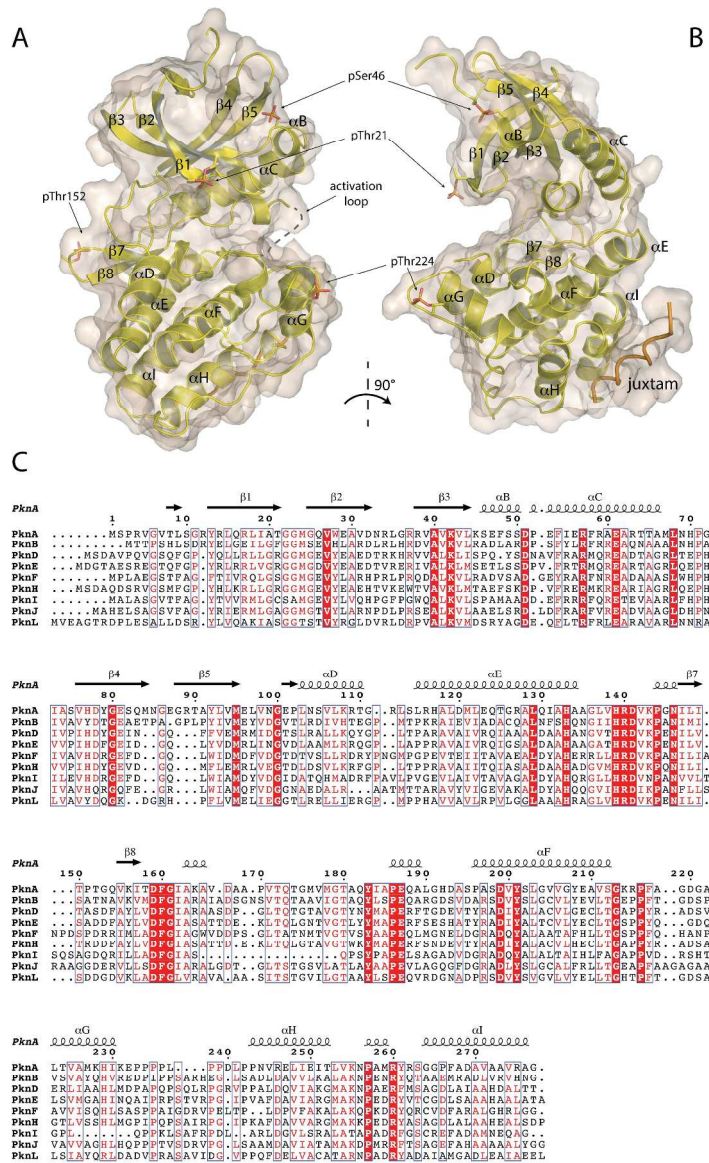


Fig. 1. (A, B) Cartoon representation of the overall structure of the catalytic domain of PknA in unliganded form; secondary structure elements are indicated. The modeled portion of the juxtamembrane segment, which folds as a left-handed PPII helix, is shown in orange. The phosphorylated residues identified in electron density maps are indicated. (C) Sequence alignment of the N-terminal catalytic domains of the transmembrane receptor *M. tuberculosis* kinases PknA, PknB, PknD, PknE, PknF, PknH, PknI, PknJ, PknL that all share the same domain topology^{3, 19}; PknG and PknK, which are soluble kinases, are omitted. The secondary structure elements of the catalytic domain of PknA (this work) have been depicted through ESPrpt 3.0³².

266x436mm (300 x 300 DPI)

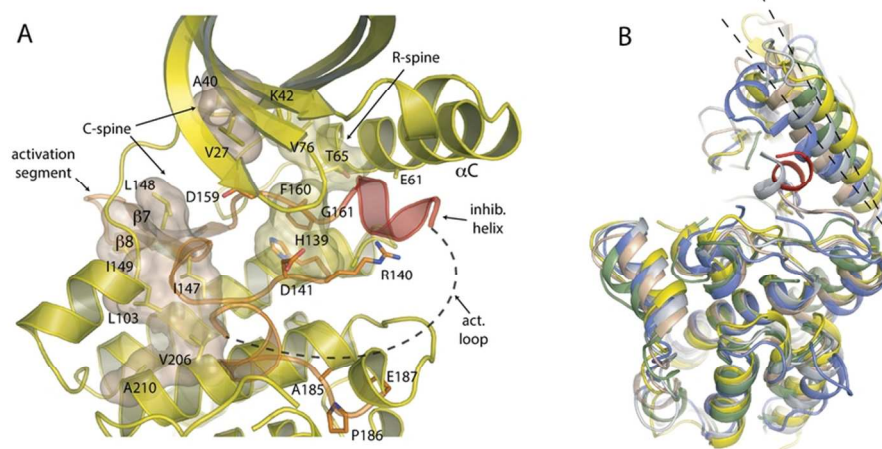


Fig. 2. (A) Close view of the active site pocket in PknA. The activation segment is highlighted in orange, and key conserved residue motifs known to be involved in the phosphorylation process or in structuring a catalytically competent kinase are shown in sticks, i.e. the motifs HRD (His139 to Asp141), DFG (Asp159 to Gly161), APE (Ala185 to Glu187). The N-terminal modeled portion of the activation loop, which is structured as a one-turn inhibitory α -helix packing against α C, is shown in red. The unassembled catalytic and regulatory spines (C-spine in light brown, R-spine in yellow) are shown with a semitransparent surface representation. See the text for details. (B) Lateral view of the superimposed catalytic domains of PknA (yellow, this study), *M. tuberculosis* PknB in complex with AMP-PCP (pdb entry 1o6y, light brown; ⁹), *M. tuberculosis* PknE (green; pdb entry 2h34, ³¹), *S. aureus* PknB (gray; pdb entry 4eqm, ²⁶) and the human cAMP-dependent kinase PKA in ternary complex with MgATP and an inhibitory peptide, shown as the paradigm of the active conformation of a Hanks-type protein kinase (purple; pdb entry 1atp, ²⁴). The dashed lines indicate the different orientation of the α C helix axis when comparing PknA (yellow) and PknB (light brown).

84x39mm (300 x 300 DPI)